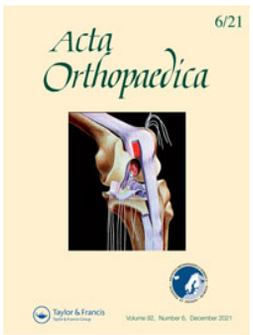

Acta Orthopaedica Scandinavica

ISSN: 0001-6470 (Print) (Online) Journal homepage: informahealthcare.com/journals/iort19

Fluorescence immunohistochemistry and confocal scanning laser microscopyA protocol for studies of joint innervation

Jean Jew, Evelyn Berger, Richard Berger & Yu-Te Lin

To cite this article: Jean Jew, Evelyn Berger, Richard Berger & Yu-Te Lin (2003) Fluorescence immunohistochemistry and confocal scanning laser microscopyA protocol for studies of joint innervation , Acta Orthopaedica Scandinavica, 74:6, 689-696, DOI: 10.1080/00016470310018216

To link to this article: https://doi.org/10.1080/00016470310018216

Fluorescence immunohistochemistry and confocal scanning laser microscopy

A protocol for studies of joint innervation

Jean Y Jew[1], Evelyn J Berger[2], Richard A Berger[2] and Yu-Te Lin[2]

[1]Department of Anatomy, University of Iowa College of Medicine, Iowa City, IA, [2]Biomechanics Laboratory, Division of Orthopedic Research, Mayo Clinic Rochester, Rochester, MN, USA
Correspondence: berger.richard@mayo.edu
Submitted 02-12-09. Accepted 03-05-24

ABSTRACT We have developed a reliable technique for labeling and examining neural structures in soft tissues associated with articular joints and have tested it in human wrist joints under various specimen-related conditions. The labeling protocol employs an immunohistochemical process with a panneuronal marker (PGP 9.5) as the primary antibody and Alexa Fluor 488 as the fluorescing secondary antibody. Imaging was done using a confocal laser scanning microscope, which produced exceptionally detailed three-dimensional images of nerve endings and transiting nerve fibers from thick sections of wrist joint ligaments obtained from human cadavers. The protocol provided a practical postmortem window for specimen acquisition and processing without significant apparent worsening of image quality. The images produced are resistant to fading with repeated exposure to a fluorescent light source, which gives many opportunities for observation. Background staining is minimal, producing high contrast labeling of target tissues, which, in turn, enhances image analysis.

Although neurons can be detected with the light microscope using general tissue stains, such preparations do not permit adequate viewing of many neuronal components. Nerve fibers and terminal axons may be difficult to distinguish from surrounding structures or missed completely in sections where they have been cut obliquely or transversely. Therefore, methods that utilize neuron-specific markers and permit visualization of the entire neuron offer significant advantages for accurate assessment of patterns, distributions and density of innervation. Silver or gold chloride techniques have historically been the commonest means of staining neural tissues (Gairns 1930, Josza et al. 1993, Backenköhler et al. 1997, McLain and Pickar 1998, Raunest et al. 1998). Because of a lack of specificity, staining with silver or gold chloride techniques may not label all neurons, and nonneuronal structures such as blood vessels may be inadvertently labeled. More recently, immunohistochemical techniques have been developed to enhance neural tissue staining specificity and image analysis potential (Brodin et al. 1988). Fundamental to a successful outcome using immunohistochemical techniques is the choice of an appropriate primary antibody that is sufficiently specific and sensitive for the desired antigen marker and of secondary antibodies with properties that optimize visualization of the antigen-antibody complex. Potential limitations with immunohistochemical techniques include targeting the wrong tissue, nonspecific background staining, degradation of the image quality over time and suboptimal image analysis. Our overall objective has been to analyze the morphology of all neural tissues in and about the wrist joint capsule. We have successfully adapted an immunohistochemical technique (Jew et al. 1996) to label and visualize the mechanoreceptor and nerve population of the anterior and posterior wrist joint capsule, using PGP 9.5 as the primary antibody and a fluorophore-conjugated

secondary antibody, followed by image analysis, using laser confocal microscopy. In this report, we describe the details of our protocol.

Material and methods

We used 4 fresh unfrozen cadavers, received within 12 hours of death, to obtain 8 radiocarpal ligaments, including the dorsal radiocarpal, radioscaphocapitate, long radiolunate and short radiolunate ligaments (Berger 2001). Specimens were screened for wrist arthropathy and generalized neurological disorders that can affect peripheral nerves. Each ligament was isolated by sharp subperiosteal dissection and immersed in a fixative solution of 4% paraformaldehyde in 0.1M phosphate buffer (PB), pH 7.4, at 4 °C for 24–48 hours. After fixation, the ligaments were washed 4 × 4 min. in 0.1 M phosphate buffered saline (PBS), pH 7.4, at 4 °C followed by a series of short washes and incubation in 0.1M PBS containing 20% sucrose buffer for cryoprotection. At this point, tissues were either prepared for cryostat sectioning, or stored at –70 °C in the 20% sucrose buffer for sectioning at a later time.

Ligament tissues were mounted and frozen in embedding media (Tissue Tek, Sakura Finetek USA Inc., Torrance, CA), taking care to record their orientation on the cryostat chuck. This enabled us to register each section for serial analysis. Using a cryostat, serial sections were cut at 50 μm thickness and mounted on super (+) charged glass slides. The slides were placed in holders and air-dried overnight at room temperature.

Sections were encircled with PAP PEN (Research Products International Corp., Mt. Prospect, IL) to form a barrier to keep solutions on the tissue sections, and slides were placed in a humidity box during processing to minimize evaporation of solution. The sections were washed 4 × 15 minutes with cold 0.1M PBS containing 3% Triton X-100 (TX-100) (Fisher Scientific, Hanover Park, IL) followed by incubation for 2 hours at room temperature in blocking solution, consisting of 4% normal goat serum (Sigma, St. Louis, MO), 0.25% bovine serum albumin (Jackson ImmunoResearch Laboratories Inc., Westgrove, PA), and 2% TX-100, all in 0.1 M PBS. Tissues were then washed 4 × 15 minutes in cold 0.1M PBS and incubated in primary antibody for 18–20 hours at 4 °C. The primary antibody was anti- protein gene product 9.5 (PGP 9.5) (rabbit antibody to human PGP 9.5, Accurate Chemicals and Scientific Corporation, Westbury, NY) diluted 1:400 in a diluent solution consisting of 0.5% TX-100 in 0.1 M PBS. After incubation at 4 °C, tissues continued to incubate for another 2 hours at room temperature. After 4 × 15 minute washes in cold 0.1 M PBS, the sections were incubated in the dark for 11/2 hours at room temperature, in secondary antibody conjugated to a fluorescent tag (Alexa Fluor 488 goat anti-rabbit IgG, Molecular Probes, Eugene, OR) diluted 1:200 with the same diluent used for the primary antibody. Sections were then given a series of washes, during which they were kept covered to minimize exposure to light: 4 × 10 minutes in cold 0.1 M PBS, 1 × 20 minutes in cold 0.05 M PB, and a final quick rinse in double-distilled H2O before cover slipping with Vectashield (Vector Laboratories, Burlington, CA). Cover slips were sealed with clear nail polish and slides were stored at –70 °C until viewed with the microscope.

We examined the specimens with a confocal laser scanning microscope system (LSM-510, Carl Zeiss Inc., Thornwood, NY), using a krypton/argon laser and mounted on a motorized Axiovert 100 M microscope (Carl Zeiss Inc., Thornwood, NY) equipped for epifluorescence. Sections were viewed first with epifluorescence, using filter sets optimal for the excitation (490–494 nm) and emission (520–525 nm) wavelengths of Alexa Fluor 488. Each section was examined at low magnification (10×) for orientation of tissues and to map locations of pertinent structures, which were recorded and drawn on templates representing the sections and their positions relative to the ligament. When labeled mechanoreceptors or other pertinent structures were identified, they were then viewed with 40× and 63× objectives to obtain more detailed information and to determine whether the field should be scanned with confocal microscopy. The microscope was switched to the laser scanning mode by setting up the LSM software-controlled scan module (Kontron KS400 Image Analyzer Workstation, Carl Zeiss Inc., Thornwood, NY). Multiple sections were scanned to establish settings for obtaining optimal mechanoreceptor

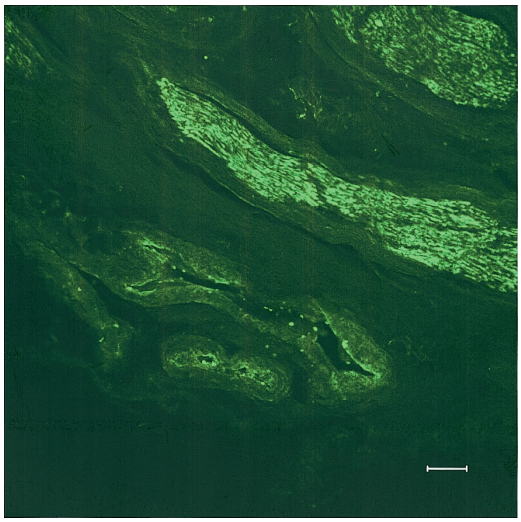

Figure 1. A confocal microscope z-series showing an oblique section of a median nerve immunolabeled for PGP 9.5. In the upper right part of the micrograph, two nerve fascicles contain the bright fluorescent green label. Surrounding structures are dark and show no specific immunolabeling except for traces of nerves associated with blood vessels in the lower part of the photo. — = 100 µm

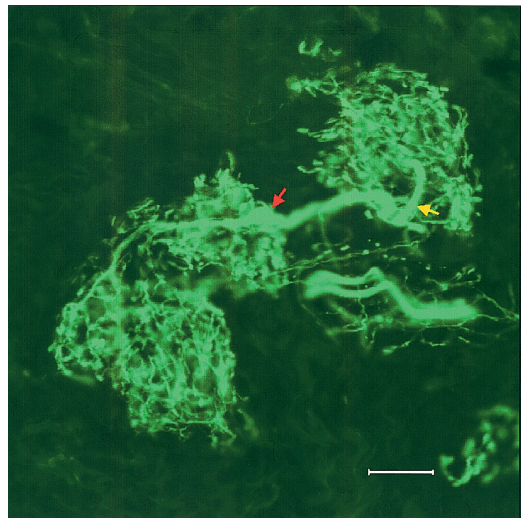

Figure 2. This confocal z-series photomicrograph shows a cluster of two type I mechanoreceptors from the DRC ligament. The mechanoreceptor on the right measures 160 × 120 µm in size; its attached afferent nerve fiber (yellow arrow) is 7.0µm in diameter, and the terminal fibers comprising the receptor range from 2.5–3.0 µm in diameter. The nerve fiber configurations in the middle and on the left are actually one mechanoreceptor, measuring 300 × 120 µm, with an afferent nerve (red arrow) diameter of 8.0 µm, and terminal fiber diameters of 2.0–2.5 µm. — = 50 µm

and nerve images for qualitative and quantitative analysis. After these settings were determined, they were saved and the configuration was used for acquisition and analysis of all images in the study to ensure consistency and valid comparisons both within the same section, and between different sections and specimens. Configurations were standardized for parameters such as: excitation wavelength (488 nm); pinhole size; resolution; total thickness of tissue section from which optical sections were to be collected; thickness of each optical section; and number of optical sections to be scanned. Optical sections were then "stacked" or merged to create high resolution "z-series" images that permitted 3-dimensional (3D) visualization of the entire mechanoreceptor or nerve. The acquired data were sent directly to a PC-controlled workstation.

Using LSM software functions, images were analyzed in 2-D and 3-D modes to provide quantitative data—e.g., length and diameter of mechanoreceptors and terminal axons—and manipulated and rotated to determine receptor, nerve and target relationships, and mechanoreceptor classification.

Results

The image quality of the preparations was excellent and consistent in all specimens. The intensity of fluorescence, precision of immunolabeling, and clear contrast between labeled nerves and receptors and background were excellent. With epifluorescence, nerves (Figure 1) and nerve receptors containing the Alexa Fluor label appeared bright green against the dark background of unlabeled structures surrounding them. Fine morphological details of nerves and especially of nerve endings, not usually discernible with the resolution of conventional light microscopy, were visible and could be tracked readily through adjacent serial sections. Thus, there was minimal ambiguity regarding the identification, quantification and classification of mechanoreceptors (Figure 2). Our preparations showed little or no background and nonspecific staining. Nervous elements were brightly labeled and easily distinguished from unlabeled structures such as blood vessels, collagen, elastin, and other connective tissue elements.

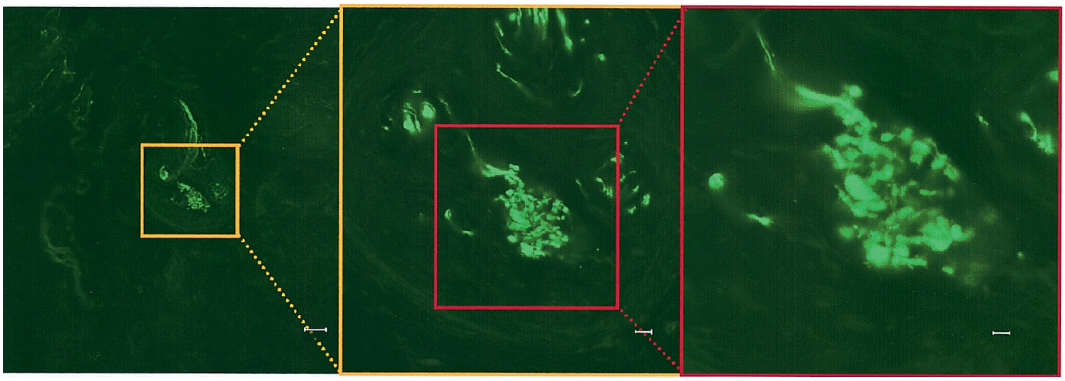

Figure 3. In this sequence of fluorescent confocal photomicrographs, the left panel (— = 50 µm) shows a type I mechanoreceptor from the DRC ligament as viewed with a 10× objective. Using the digital zoom feature of the laser confocal scope, the 40X image (center, — = 10 µm) is enlarged to 80× (right, — = 5 µm). Digital zoom resizing maintained scalar relationships and did not affect the quality of resolution needed to obtain accurate and consistent measurements of receptor and nerve fiber sizes.

Structures labeled with the fluorochrome used in this protocol, Alexa Fluor 488, retained their bright fluorescence intensity for several months when stored in the freezer. Details of images remained sharp and bright throughout the analysis.

Using laser confocal microscopy, the quality of image resolution enabled us to measure structures as small as the terminal fibers comprising mechanoreceptors (Figure 2). For detailed analyses and measurements, confocal images were usually examined and collected using 40× magnification. However, it was sometimes advantageous to enlarge or reduce the image—e.g., to enhance accuracy in tasks requiring computer-assisted tracing and measuring. The zoom features of the laser confocal system provided the versatility needed to enlarge or reduce the size of a structure or field without having to retrieve and rescan the tissue section (Figure 3). The optical sections generated by the confocal microscope system and the z- stack mode were particularly useful for these studies of joint innervation because the structure, organization, and relationships of individual elements could be discerned in the complex jumble of terminal fibers and nerves that formed one receptor or clusters of receptors (Figures 2 and 4). The enhanced visualization of details through the entire thickness of the structure made it possible to convert optical sections and z-stacks to 3-D images that could be manipulated and rotated to view mechanoreceptor structure and relationships in a virtual 3-D environment (Figure 5).

Discussion

The distribution and morphological appearance of nerve endings in the soft tissues surrounding articular joints are sparsely documented, and various investigators may report, in the same tissue, seemingly contradictory descriptions of receptor identification and distribution (Freeman and Wyke 1967, Kennedy et al. 1974, Kennedy et al. 1982, Goertzen et al. 1992, Koch et al. 1995). Such circumstances are due in no small part to the technical difficulties in adequately visualizing and identifying the different nerve components in the ligaments or articular soft tissues.

Most neuron's processes are so extensive that only part of the cell is present in a tissue section that is thin enough for most types of conventional light microscopy—i.e., 8–40 μm. Since encapsulated joint receptors may range from 40–600 μm in length and 40–100 μm in diameter, only portions of nerves and nerve terminals may be present in a single tissue section. Therefore, their identification and classification require (1) use of tissue stains that permit differentiation of nerve from other tissue elements and (2) systematic analysis of serial sections.

Although it is possible to identify neural elements with standard staining techniques, the lack of nerve-specific staining makes identification of many terminals and receptors equivocal, thereby impeding quantification and interpretation of receptor type. The first attempts to visualize

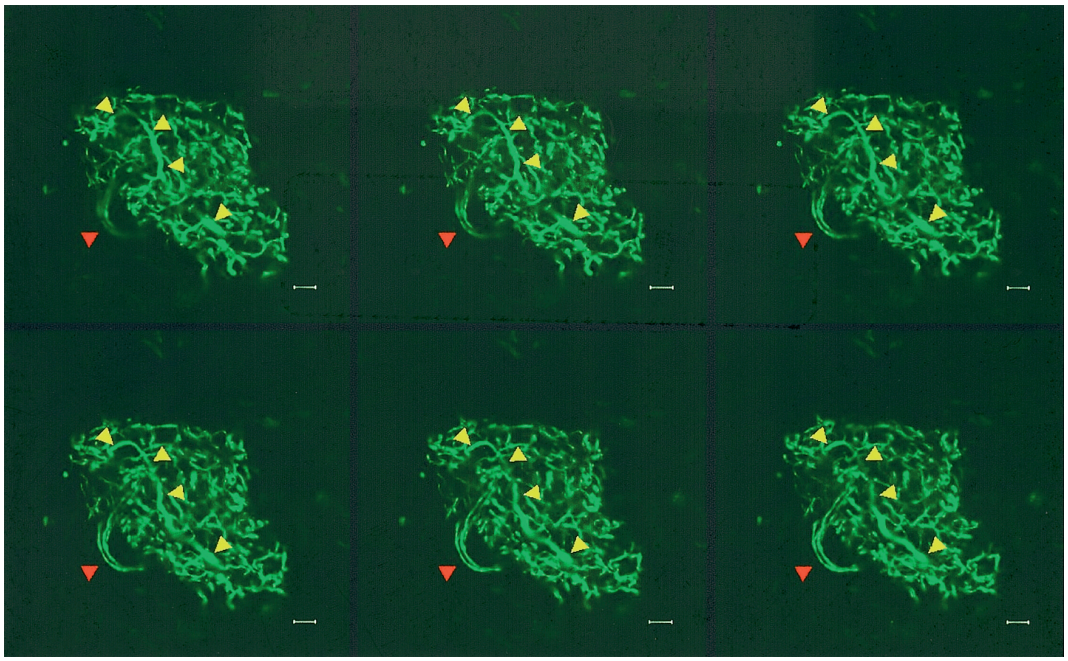

Figure 4. Series of micrographs of a single type I mechanoreceptor from a DRC ligament. Each panel in the series is an optical section taken at a different level through the thickness of the mechanoreceptor. The identities and relationships of a number of structures become apparent or are clarified only when several or all the panels are considered together, i.e., as in a z-stack. The nerve fiber in the center of the mechanoreceptor (yellow arrows) can be traced and shown to lead to the mechanoreceptor. The nerve fibers in the left lower corner (red arrows) pass close to the mechanoreceptor, but are not one of its components. — = 20 µm

neurons and their terminals more specifically employed silver- or gold-chloride techniques, modifications of which are still widely used today.

Because of the affinity of nerve cells and their processes for silver solutions (argyrophilia), silver impregnation methods (Golgi 1873, Cajal 1911) stained nerve cell bodies and larger dendrites, axons, and synapses, due to their neurofibrillar content, and were particularly valuable for the study of motor and sensory nerve endings (Bielchowsky 1902, Bodian 1936). However, these silver methods are capricious and require extensive experience to obtain good tissue preparations.

Gold chloride impregnation, because of its ability in optimally-stained sections to show fine anatomic detail, is currently a preferred method for studies of receptor type, density, and distribution in the sensory innervation of articular tissues. Studies of human joint tissue using the gold chloride technique have included the elbow collateral ligaments (Petrie et al. 1998), knee anterior cruciate ligament (Georgoulis et al. 2001), palmar wrist ligaments (Petrie et al. 1997), lumbar and thoracic facet joint capsules (McLain and Pickar 1998), metacarpophalangeal collateral ligaments (Sathian and Davanandan 1983), myotendinous junctions (Jozsa et al. 1993), and posterior sacroiliac ligaments (Vilensky et al. 2002). However, the appearance of stained structures may vary both within a section and between samples, and, since nonneural structures are also stained, nerves and nerve endings must be distinguished from other structures on the basis of their anatomical features. Sometimes this is problematic (De Avila et al. 1989, Koch et al. 1995, McLain and Pickar 1998) and may account for the apparent contradictions in articular innervation reported by several investigators. A modification of the gold chloride technique was reported using frozen tissue processing, but the nonspecific staining of the gold chloride methods remains a significant limitation (Raunest et al. 1998, Zimny 1988).

The use of immunohistochemical techniques and the development of commercially available antibodies to cellular constituents have greatly improved the ability to identify specific structures

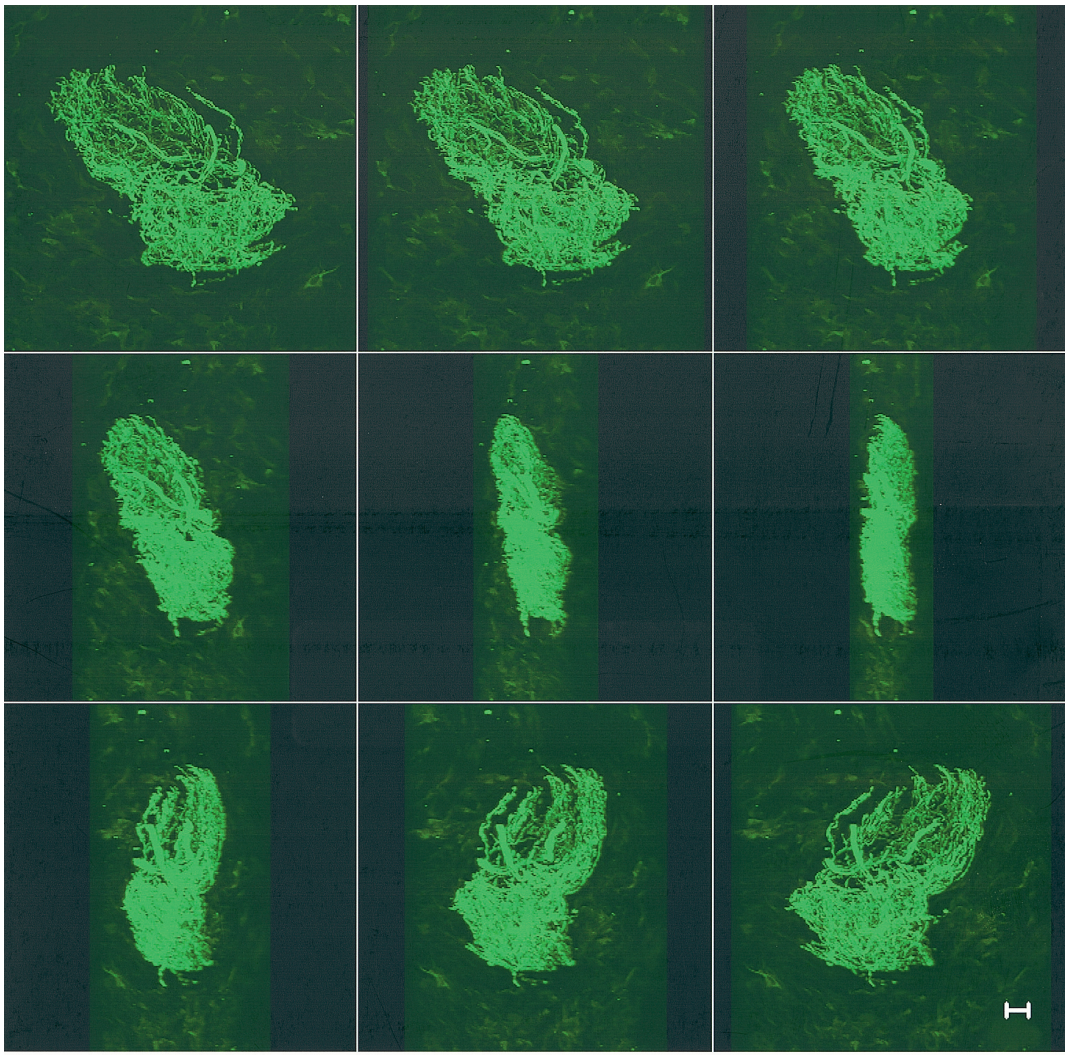

Figure 5. A series of confocal microscopy images showing a mechanoreceptor from a DRC ligament. Merging of optical sections using "z-series" provides a 3D-reconstruction image that can be rotated to view the entire mechanoreceptor from different angles and planes. — = 20 µm

and obtain information about their morphology, distribution, and relationships to other structures in their microenvironment. As regards neurons and their components, a number of antibody markers are commercially available for visualizing and classifying them according to certain criteria.

Antibodies to substance P (SP) (Korkala et al. 1985, Beaman et al. 1993, Vilensky et al. 2002), calcitonin gene-related peptide (CGRP) (Jang et al. 2000) and neurofilament protein (NFP) (Rhalmi et al. 1993) have been used by other investigators in recent articular mechanoreceptor studies. Although SP and CGRP are neurotransmitters/neuromodulators found in sensory nerves carrying nociceptive information, their presence in mechanoreceptors has not been established. From previous experience in our laboratory, use of antibody to NFP did not result in the panneuronal staining necessary for our study. Therefore, we selected immunohistochemical localization of the panneuronal marker PGP 9.5 to label nerves and nerve terminals in our studies of mechanoreceptor density and distribution in the ligaments of the wrist. PGP 9.5 is a neural cytoplasmic protein known as ubiquitin carboxyl terminal hydrolase and has been used successfully in studies of the innerva-

tion of intervertebral discs (Palmgren et al. 1999, Roberts et al. 1995), rat synovium (Hukkanen et al. 1992), and human knee synovium (Hirasawa et al. 2000).

In brightfield light microscopic immunohistochemistry, antibody-linked enzyme complexes, such as PAP (Sternberger 1979) or ABC (Hsu et al. 1981), are combined with a substrate to produce a colored reaction product to label the antigen marker in nerves and nerve terminals. The reaction product is stable, and the slide can be examined at any time and stored indefinitely. With fluorescence immunohistochemistry, nerves are labeled with a fluorophore, which, in our protocol, is conjugated to the secondary antibody. Fluorescent labels will fade, especially when exposed to light, and tissues are best viewed within days of completion of processing and mounting. The protocol that we propose in this report is a modification of that used by Jew et al. (1996) for whole mounts of autonomic nerves in which antibodies, washes, diluents, fluorophores, mounting media, and processing techniques have been selected/developed to yield images with strong fluorescent signals that resist fading and deterioration for several weeks.

The major advantage of using fluorescence labeling to localize nerves and nerve terminals in our experimental model is the ability to analyze the tissue with the laser confocal scanning microscope. In conventional microscopy, thick tissue sections produce an image that represents the sum of sharp image details from the plane of the section that is in focus, combined with blurred images from all of the planes that are out of focus. At magnifications necessary to view details of nerves and nerve terminals, tissue sections greater than three to five microns produce images in which most of the light is contributed by regions that are not in focus. Contrast and resolution are reduced because of the contribution from a blurred background that is superimposed over the weaker in-focus image.

The laser scanning confocal microscope, by using pinhole apertures to limit the specimen focal plane, in effect produces an image that comes from a thin section of tissue—i.e., an "optical section". Due to this pinhole collimation technology designed into the scanning system, and the ultra-high resolution offered by the laser light source and its high signal-to-noise ratio, tissue sections as thick as 200 μm (Brodin et al. 1988) can be viewed as a series of optical sections. Fine structural details are easily distinguished, and the resolution of images obtained through the confocal microscope is excellent (Brodin et al. 1988, Brakenhoff et al. 1989, Shotton and White 1989). Moreover, these optical images can be reassembled with minimal deterioration of contrast to obtain three-dimensional reconstructions of pertinent structures—e.g., the entire thickness of nerve or the major portion of a receptor ending. The enhanced structural detail and ability to visualize most of, if not the entire, nerve or a receptor facilitate greater accuracy in detecting, interpreting, and quantifying articular receptors.

In summary, we have found that (1) the immunohistochemistry protocol, in which antibody to PGP 9.5 and a secondary antibody conjugated to the fluorophore, Alexa Fluor 488, are used to label nerves and nerve terminals, combined with (2) image analysis with laser scanning confocal microscopy, is a reliable and optimal technique for studies of sensory innervation in articular tissues. As used in our studies, there is minimal nonspecific staining, exceptional longevity of fluorescent label, excellent resolution of morphologic details at optical magnification levels, and the capability of generating three-dimensional constructs of serial sections to produce a composite "map" of neural anatomy of the tissue being studied.

This study was supported by the following grants: NIH AR 47806, NIH NS 39771, and Juvenile Diabetes Foundation International (JDFI) 1-2000-291.

Backenköhler U, Strasmann T J, Halata Z. Topography of mechanoreceptors in the shoulder region. A computer-aided 3D reconstruction in the laboratory mouse. Anat Rec 1997; 248: 433-41.

Beaman D N, Graziano G P, Glover R A, Wojtys E M, Chang V. Substance P innervation of lumbar spine facet joints. Spine 1993; 18: 1044-9.

Berger R A. The anatomy of the ligaments of the wrist and distal radioulnar joint. Clin Orthop 2001; 383: 32-40.

Bielchowsky M. Die Silberimpragnation der Axencylinder. Neurol Zbl 1902; 21: 579-84.

Bodian D. A new method for staining nerve fibers and nerve endings in mounted paraffin sections. Anat Rec 1936; 65: 89-97.

Brakenhoff G J, van der Voort H T M, van Spronsen E A, Nanninga N. Three-dimensional imaging by confocal scanning fluorescence microscopy. J Microsc 1989; 153: 151-9.

Brodin L, Ericsson M, Mossberg K, Hokfelt T, Ohta Y, Grillner S. Three-dimensional reconstruction of transmitter-identified central neurons by "en bloc" immunofluorescence histochemistry and confocal scanning microscopy. Exp Brain Res 1988; 73: 441-6.

Cajal S R. 1911, Histologie du système nerveux de l'homme et des vertebres, Paris: Maloine; Edition Francaise Revue: Tome I, 1952; Madrid: Consejo Superior de Investigaciones Cientificas.

De Avila G A, O'Connor B L, Visco D M, Sisk T D. The mechanoreceptor innervation of the human fibular collateral ligament. J Anat 1989; 162: 1-7.

Freeman M A, Wyke B. The innervation of the ankle joint. An anatomical and histological study in the cat. Acta Anat 1967; 68: 321-33.

Gairns F. Modified gold chloride method for the demonstration of nerve endings. Q J Microsc Sci 1930; 74: 151-5.

Georgoulis A D, Pappa L, Moebius U, Malamou-Mitsi V, Pappa S, Papageorgiou C O, et al. The presence of proprioceptive mechanoreceptors in the remnants of the ruptured ACL as a possible source of re-innervation of the ACL autograft. Knee Surg Sports Traumatol Arthrosc 2001; 9: 364-8.

Goertzen M, Gruber J, Dellmann A, Clahsen H, Schulitz K-P. Neurohistological findings after experimental anterior cruciate ligament allograft transplantation. Arch Orthop Trauma Surg 1992; 111: 126-9.

Golgi C. Sulla struttura della sostanza grigia del cervello. Gaz Med Ital Lombardia 1873; 6: 244-6.

Hirasawa Y, Okajima S, Ohta M, Tokioka T. Nerve distribution to the human knee joint: anatomical and immunohistochemical study. Int Orthop 2000; 24: 1-4.

Hsu S M, Raine L, Fanger H. Use of avidin-biotin-peroxidase complex (ABC) in immunoperoxidase techniques: a comparison between ABC and unlabeled antibody (PAP) procedures. J Histochem Cytochem 1981; 29: 577-80.

Hukkanen M, Konttinen Y T, Rees R G, Santavirta S, Terebghi G, Polak J M. Distribution of nerve endings and sensory neuropeptides in rat synovium, meniscus and bone. Int J Tiss React 1992; 14: 1-10.

Jang Y C, Isik F F, Gibran N S. Nerve distribution in hemangiomas depends on the proliferative state of the microvasculature. J Surg Res 2000; 93: 144-8.

Jew J Y, Fink C A, Williams T H. Tyrosine hydrolase- and nitric oxide synthase-immunoreactive nerve fibers in mitral valve of young adult and aged Fischer 344 rats. J Auton Nerv Syst 1996; 58: 35-43.

Jozsa L, Balint J, Kannus P, Jarvinen M, Lehto M. Mechanoreceptors in human myotendinous junction. Muscle Nerve 1993; 16: 453-7.

Kennedy J C, Weinberg H W, Wilson A S. The anatomy and function of the anterior cruciate ligament. J Bone Joint Surg (Am) 1974; 56: 223-35.

Kennedy J C, Alexander I J, Hayes K C. Nerve supply of the human knee and its functional importance. Am J Sports Med 1982; 10: 329-35.

Koch B, Kurriger G, Brand R A. Characterisation of the neurosensory elements of the feline cranial cruciate ligament. J Anat 1995; 187: 353-9.

Korkala O, Grönblad M, Liesi P, Karaharju E. Immunohistochemical demonstration of nociceptors in the ligamentous structures of the lumbar spine. Spine 1985; 10: 156-7.

McLain R F, Pickar J G. Mechanoreceptor endings in human thoracic and lumbar facet joints. Spine 1998; 23: 168-73.

Palmgren T, Grönblad M, Virri J, Kappa E, Karaharju E. An immunohistochemical study of nerve structures in the annulus fibrosus of human normal lumbar intervertebral discs. Spine 1999; 24: 2075-9.

Petrie S, Collins J, Solomonow M, Wink C, Chuinard R. Mechanoreceptors in the palmar wrist ligaments. J Bone Joint Surg (Br) 1997; 79: 494-6.

Petrie S, Collins JG, Solomonow M, Wink C, Chuinard R, D'Ambrosia R. Mechanoreceptors in the human elbow ligaments. J Hand Surg 1998; 23A: 512-8.

Raunest J, Sager M, Burgener E. Proprioception of the cruciate ligaments: Receptor mapping in an animal model. Arch Orthop Trauma Surg 1998; 118: 159-63.

Rhalmi S, Yahia L H, Newman N, Isler M. Immunohistochemical study of nerves in lumbar spine ligaments. Spine 1993; 18: 264-7.

Roberts S, Eisenstein S M, Menage J, Evans E H, Ashton I K. Mechanoreceptors in intervertebral discs. Morphology, distribution, and neuropeptides. Spine 1995; 20: 2645-51.

Sathian K, Devanandan M S. Receptors of the metacarpophalangeal joints: a histological study in the bonnet monkey and man. J Anat 1983; 137: 601-3.

Shotton D, White N. Confocal scanning microscopy: three-dimensional biological imaging. Trends Biochem Sci 1989; 14: 435-9.

Sternberger L A. The unlabeled antibody (PAP) method. J Histochem Cytochem 1979; 27: 1657-9.

Vilensky J A, O'Connor B L, Fortin J D, Merkel G J, Jimenez A M, Scofield B A, Kleiner J B. Histologic analysis of neural elements in the human sacroiliac joint. Spine 2002; 27: 1202-7.

Zimny M L. Mechanoreceptors in articular tissues. Am J Anat 1988; 182: 16-32.